

# General Light-Mediated, Highly Diastereoselective Piperidine Epimerization: From Most Accessible to Most Stable Stereoisomer

Zican Shen,<sup>§</sup> Morgan M. Walker,<sup>§</sup> Shuming Chen, Giovanny A. Parada, Duc M. Chu, Sun Dongbang, James M. Mayer,<sup>\*</sup> K. N. Houk,<sup>\*</sup> and Jonathan A. Ellman<sup>\*</sup>



Cite This: *J. Am. Chem. Soc.* 2021, 143, 126–131



Read Online

ACCESS |

Metrics & More

Article Recommendations

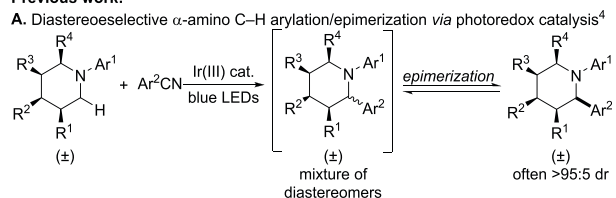
Supporting Information

**ABSTRACT:** We report a combined photocatalytic and hydrogen atom transfer (HAT) approach for the light-mediated epimerization of readily accessible piperidines to provide the more stable diastereomer with high selectivity. The generality of the transformation was explored for a large variety of di- to tetrasubstituted piperidines with aryl, alkyl, and carboxylic acid derivatives at multiple different sites. Piperidines without substitution on nitrogen as well as *N*-alkyl and aryl derivatives were effective epimerization substrates. The observed diastereoselectivities correlate with the calculated relative stabilities of the isomers. Demonstration of reaction reversibility, luminescence quenching, deuterium labeling studies, and quantum yield measurements provide information about the mechanism.

Piperidines represent the most prevalent class of heterocycles found in U.S. Food and Drug Administration approved pharmaceuticals,<sup>1</sup> and due to the importance of this motif a variety of strategies have been developed for their stereoselective synthesis and functionalization.<sup>2,3</sup> Recently, our group reported the photoredox catalyzed diastereoselective  $\alpha$ -amino C–H arylation of densely functionalized piperidine derivatives (Scheme 1A).<sup>4</sup> Key to the high diastereoselectivity of this transformation was an *in situ*, reversible photoredox-mediated  $\alpha$ -amino epimerization reaction.

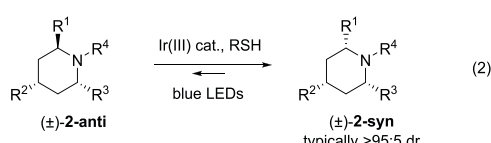
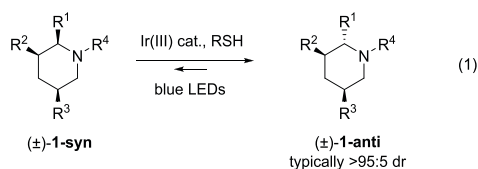
## Scheme 1. Photoredox-Mediated Piperidine Epimerization

Previous work:



This work:

B. Light-mediated epimerization of di- to tetrasubstituted piperidines to form the more stable isomer



We sought to more broadly apply light-mediated, highly diastereoselective epimerization to piperidines with a range of substitution patterns. The most extensively used methods for piperidine synthesis as well as some of the most exciting new methods often proceed with high selectivity for the contra-thermodynamic diastereomer.<sup>3b,5</sup> We speculated that epimerization through an  $\alpha$ -amino radical intermediate might provide rapid access to the more stable isomer.<sup>6</sup> However, few examples of stereoselective light-mediated epimerization have been reported.<sup>7</sup>

Herein, we describe a combined photocatalytic and hydrogen atom transfer (HAT) approach to furnish thermodynamically more stable piperidine derivatives by epimerization of the corresponding readily accessible but less stable stereoisomers. The approach was first demonstrated by highly diastereoselective epimerization of di- to tetrasubstituted contra-thermodynamic piperidines **1-syn** (Scheme 1B, eq 1), prepared by *syn* selective hydrogenation of pyridines, which is one of most extensively used methods for piperidine synthesis.<sup>5</sup> The approach was then extended to the highly diastereoselective epimerization of di- to trisubstituted contra-thermodynamic derivatives **2-anti** (Scheme 1B, eq 2), which can be obtained by Seidel and co-workers' powerful approach for diastereoselective  $\alpha$ -substitution of free piperidines.<sup>3b</sup> Epimerization was effective for piperidines with aryl, alkyl, amino, aniline, ester, and primary or tertiary amide substituents. Additionally, piperidines without substitution on nitrogen as well as *N*-alkyl and aryl derivatives were effective

Received: November 17, 2020

Published: December 29, 2020



Table 1. Scope for Conversion of 1-syn to 1-anti<sup>a</sup>

2,3-Substituted piperidines		2,5-Substituted piperidines		2,3,5-Substituted piperidines			
	<b>1a-anti</b> 91%, 98:2 dr (>99%, 98:2 dr)		<b>1a-anti</b> 96%, >99:1 dr (>99%, 98:2 dr)		<b>1b-anti<sup>b</sup></b> 86%, 98:2 dr (>99%, 95:5 dr)		<b>1c-anti</b> 81%, 97:3 dr (87%, 97:3 dr)
	<b>1d-anti<sup>c,d,e</sup></b> 98%, 95:5 dr (>99%, 90:10 dr)		<b>1e-anti<sup>d</sup></b> 95%, 93:7 dr (>99%, 91:9 dr)		<b>1f-anti<sup>f</sup></b> 88%, 92:8 dr (89:11 dr)		<b>1g-anti</b> 96%, 97:3 dr (>99%, 97:3 dr)
	<b>1h-anti</b> 98%, 95:5 dr (>99%, 92:8 dr)		<b>1i-anti<sup>g</sup></b> 97%, >99:1 dr (>99%, 95:5 dr)		<b>1j-anti<sup>c</sup></b> 98%, 85:15 dr (>99%, 83:17 dr)		<b>1k-anti<sup>c</sup></b> 58%, >99:1 dr (68%, 97:3 dr)
	<b>1l-anti<sup>b</sup></b> 75%, 97:3 dr (85%, 97:3 dr)		<b>1m-anti<sup>b</sup></b> 91%, 97:3 dr (98%, 97:3 dr)		<b>1n-anti<sup>b,h</sup></b> 79%, 95:5 dr (>99%, 95:5 dr)		<b>1o-anti<sup>b,h</sup></b> 95%, 78:22 dr (>99%, 78:22 dr)
	<b>1p-anti<sup>i</sup></b> 93%, 97:3 dr (>99%, 97:3 dr)		<b>1q-anti<sup>c,j</sup></b> 90%, >99:1 dr (>99%, 93:7 dr)		<b>1r-anti<sup>b,k</sup></b> 77%, 97:3 dr (>99%, 92:8 dr)		<b>1s-anti<sup>b</sup></b> 83%, >99:1 dr (95%, 92:8 dr)
	<b>1t-anti<sup>d</sup></b> 90%, 95:5 dr (>99%, 95:5 dr)		<b>1u-anti</b> 89%, 97:3 dr (98%, 92:8 dr)		<b>1v-anti</b> 91%, >99:1 dr (98%, >99:1 dr)		<b>1w-anti</b> 94%, 93:7 dr (97%, 92:8 dr)

<sup>a</sup>Isolated yields on 0.3 mmol scale; dr was determined by <sup>1</sup>H NMR analysis. Crude yields and dr are noted in parentheses and were determined by <sup>1</sup>H NMR analysis with an external standard. <sup>b</sup>MeCN as solvent. <sup>c</sup>CySH instead of PhSH. <sup>d</sup>40 h reaction time. <sup>e</sup>1d-syn was an 88:12 mixture of diastereomers. <sup>f</sup>Isolated yield on 0.1 mmol scale. <sup>g</sup>Reaction performed at 0.03 M due to poor solubility. <sup>h</sup>Isolated yield on 0.2 mmol scale. <sup>i</sup>1p-syn was a 63:37 syn/anti mixture of diastereomers. <sup>j</sup>1q-syn was a 60:40 syn/anti mixture of diastereomers. <sup>k</sup>1r-syn was a 66:34 syn/anti mixture of diastereomers.

epimerization substrates. The experimentally observed diastereomer ratios are generally in reasonable agreement with the calculated relative stability of the two diastereomers, which is helpful for predicting epimerization selectivity. Moreover, quantum yield determination, luminescence quenching, and deuterium labeling studies provide insight into the mechanism for epimerization.

We began our investigation by exploring photocatalytic epimerization of **1a-syn** (see Tables S1 and S2 for optimization experiments). High diastereoselectivity for **1a-anti** was achieved by employing 1 mol%  $[\text{Ir}\{\text{dF}(\text{CF}_3)\text{ppy}\}_2(\text{dtbpy})]\text{PF}_6$  photocatalyst and 1.0 equiv of PhSH as an HAT<sup>8</sup> reagent in acetonitrile or methanol under blue light irradiation, with methanol providing slightly higher selectivity. Control experiments revealed that photocatalyst, light, and PhSH are all necessary reaction components, with minimal (<5%) **1a-anti** obtained in their absence. A variety of hydrogen atom donors were evaluated with aromatic thiols determined to provide the highest selectivity for this substrate (Table S2). To demonstrate the scalability of this transformation, the reaction of **1a-syn** was set up on 1 mmol scale to afford **1a-anti** in 96% isolated yield and with >99:1 dr, which compares favorably to the standard 0.3 mmol reaction scale (Table 1).

After identifying the optimal reaction conditions, we next evaluated the scope of epimerization (Table 1). In addition to the 2-phenyl-derivative **1a-syn**, which provided the anti isomer as determined by X-ray crystallography, different substituents could also be incorporated on the phenyl ring. Piperidines with both electron-rich (**1b-anti**) and electron-deficient (**1c-anti**) *para* substituents were obtained with high diastereoselectivities. Epimerization of piperidine **1d-syn** with an *ortho*-substituted phenyl group gave only modest diastereoselectivity under the standard reaction conditions (data not shown), perhaps because steric interactions with the *ortho*-methyl group<sup>9</sup> prevent resonance stabilization of the  $\alpha$ -amino radical intermediate (vide infra). In contrast, use of CySH<sup>10</sup> and a longer reaction time provided **1d-anti** in 95:5 dr.

Piperidine derivatives with various functionalities at the 3-position were also explored. Piperidines displaying esters at this site epimerized to the anti product in high yields and with high diastereoselectivities (**1e-anti** and **1f-anti**). Notably, **1f-syn**, which incorporates an *N*-cyclopentyl aniline, is a late stage intermediate in the synthesis of the phase III clinical candidate avacopan.<sup>11</sup> A homologated ethyl ester (**1g-anti**), the corresponding tertiary amide (**1h-anti**), and the primary amide (**1i-anti**) all epimerized in high yields and with excellent diastereoselectivities.

When alkyl substituents were present at the 2-position, the products were obtained with good anti selectivity, including for cyclohexyl (**1j-anti**) and methyl (**1k-anti**) groups. However, CySH rather than PhSH was necessary to promote epimerization of these 2-alkyl substituted piperidines, presumably because its S–H bond dissociation energy matches with the C–H bond dissociation energies for those piperidines that do not provide aromatic stabilization for the  $\alpha$ -amino radical.<sup>10</sup> In contrast, PhSH with a weaker S–H bond dissociation energy resulted only in recovery of **1j-syn**.

We further extended the substrate scope by evaluating more highly substituted piperidines that also incorporated nitrogen substituents (Table 1). N-Alkyl substituted piperidines bearing methyl, ethyl, and isopropyl groups afforded products **1l-anti**, **1m-anti**, and **1n-anti**, respectively, in good yields and with consistently high diastereoselectivities. Epimerization of *N*-phenyl-substituted piperidine **1o-syn** proceeded in 95% yield, albeit with only moderate diastereoselectivity for the anti isomer. Extending the reaction time for this substrate did not improve the anti/syn isomer ratio.

Importantly,  $\alpha$ -epimerization is not limited to 2,3-disubstituted piperidines. For 2,5-disubstituted piperidines with aryl and alkyl substituents at the 2-position, epimerization also proceeded in high yields and stereoselectivities as demonstrated for **1p-anti** and **1q-anti**, respectively. Additionally, products were obtained in good yields and high diastereoselectivities for *N*-methyl (**1r-anti**) and *N*-isopropyl (**1s-anti**) piperidines with the 2,5-disubstitution pattern.

Piperidines with even higher levels of substitution also epimerized efficiently. For example, the all syn 2,3,5-trisubstituted piperidine **1t-syn** equilibrated with high selectivity and yield to **1t-anti**. The corresponding tetrasubstituted *N*-methyl (**1u-anti**) and *N*-ethyl (**1v-anti**) derivatives were similarly obtained with very high selectivity. Moreover, the 2,3,5-trisubstituted piperidine **1w-syn**, which incorporated an ester at the 3-position, also efficiently epimerized to give **1w-anti**.

To this point, only syn contra-thermodynamic piperidines had been investigated. To demonstrate the potential generality of  $\alpha$ -amino epimerization for contra-thermodynamic anti stereoisomers, we evaluated a number of 2,4- and 2,6-disubstituted piperidines **2-anti** (Table 2), prepared by an efficient new method developed by Seidel and co-workers.<sup>3b</sup> Under the standard reaction conditions, epimerization with greater than 95:5 diastereoselectivity for the syn isomer was observed for both unsubstituted and *N*-alkyl 2,4-disubstituted (**2a–2c**) and 2,6-disubstituted (**2e** and **2f**) piperidines. Only the *N*-phenyl substituted piperidine epimerized with modest diastereoselectivity to give **2d-syn**, consistent with that observed for *N*-phenyl 2,3-disubstituted piperidine **1o** (see Table 1).

To compare the diastereomer ratios obtained under photoredox conditions with the relative stabilities of the corresponding syn and anti isomers, we used density functional theory (DFT) to calculate the relative free energies of a representative set of piperidine diastereomers (Table 3). The relative energies for piperidine diastereomers for derivatives **1** with a range of different substituents correlated well with the observed high diastereomer ratios (entries 1–5). For these piperidines, the lower energy anti isomer displays both substituents in equatorial positions and the higher energy syn isomer displays one group axial, causing unfavorable 1,3-diaxial interactions. For the *N*-phenyl substituted piperidine **1o** (entry

Table 2. Representative Conversion of 2-anti to 2-syn<sup>a,b</sup>

	88%, 98:2 dr (98%, 95:5 dr)		96%, 96:4 dr (>99%, 96:4 dr)		87%, 95:5 dr (>99%, 93:7 dr)
	72%, 72:28 dr (91%, 72:28 dr)		80%, >99:1 dr (97%, 96:4 dr)		90%, >99:1 dr (94%, >99:1 dr)

<sup>a,b</sup> See footnotes *a* and *b* for Table 1.

Table 3. Experimental and Calculated Relative Energies

entry <sup>a</sup>	substrate	exptl dr anti/syn	exptl $\Delta G_{\text{syn}} - \Delta G_{\text{anti}}$ (kcal/mol)	calcd $\Delta G_{\text{syn}} - \Delta G_{\text{anti}}$ (kcal/mol)
1	<b>1a</b>	98:2	2.3	2.2
2	<b>1j</b>	83:17	0.9	1.3
3	<b>1k</b>	97:3	2.1	3.6
4	<b>1l</b>	97:3	2.1	2.8
5	<b>1p</b>	97:3	2.1	1.6
6	<b>1o</b>	78:22	0.8	1.9
7	<b>2e</b>	4:96	-1.9	-2.4

<sup>a</sup>  $\omega$ B97X-D/6-311++G(d,p), SMD (MeOH or MeCN) //  $\omega$ B97X-D/6-31G(d), SMD (MeOH or MeCN). Exptl = experimental.

6), while epimerization to the most stable diastereomer occurred, the relatively modest diastereoselectivity did not correlate that well with the calculated energy difference between the two diastereomers. For **2e** with a different substitution pattern (entry 7), reasonable agreement between the calculated energy difference and experimentally observed ratio was observed.

In the photoredox-mediated arylation of piperidines, we had previously observed that the distribution of piperidine isomers resulted from reversible light-mediated in situ epimerization of the initially formed  $\alpha$ -arylated piperidines.<sup>4</sup> To probe the reversibility of photoredox-mediated epimerization in our current study, we subjected stereoisomerically pure **1o-anti** to the reaction conditions (Figure 1a). By crude <sup>1</sup>H NMR analysis, we observed a 76:24 syn/anti diastereomer ratio favoring **1o-anti**, in very close agreement to the ratio obtained starting with **1o-syn** (see Table 1). Having each diastereomer converge to the same syn/anti ratio is consistent with a thermodynamically controlled process under the photoredox conditions of the reaction.

To gain further information on the mechanism of epimerization, we investigated deuterium incorporation for several piperidines with the reaction performed in methanol-*d*<sub>4</sub>, which results in rapid exchange of PhSH to PhSD (Figure 1b–d).<sup>12</sup> For **1a-syn** (Figure 1b) and **1p-syn** (Figure 1c), the diastereomeric products were obtained with complete deuterium incorporation at the 2- and 3-positions, but without

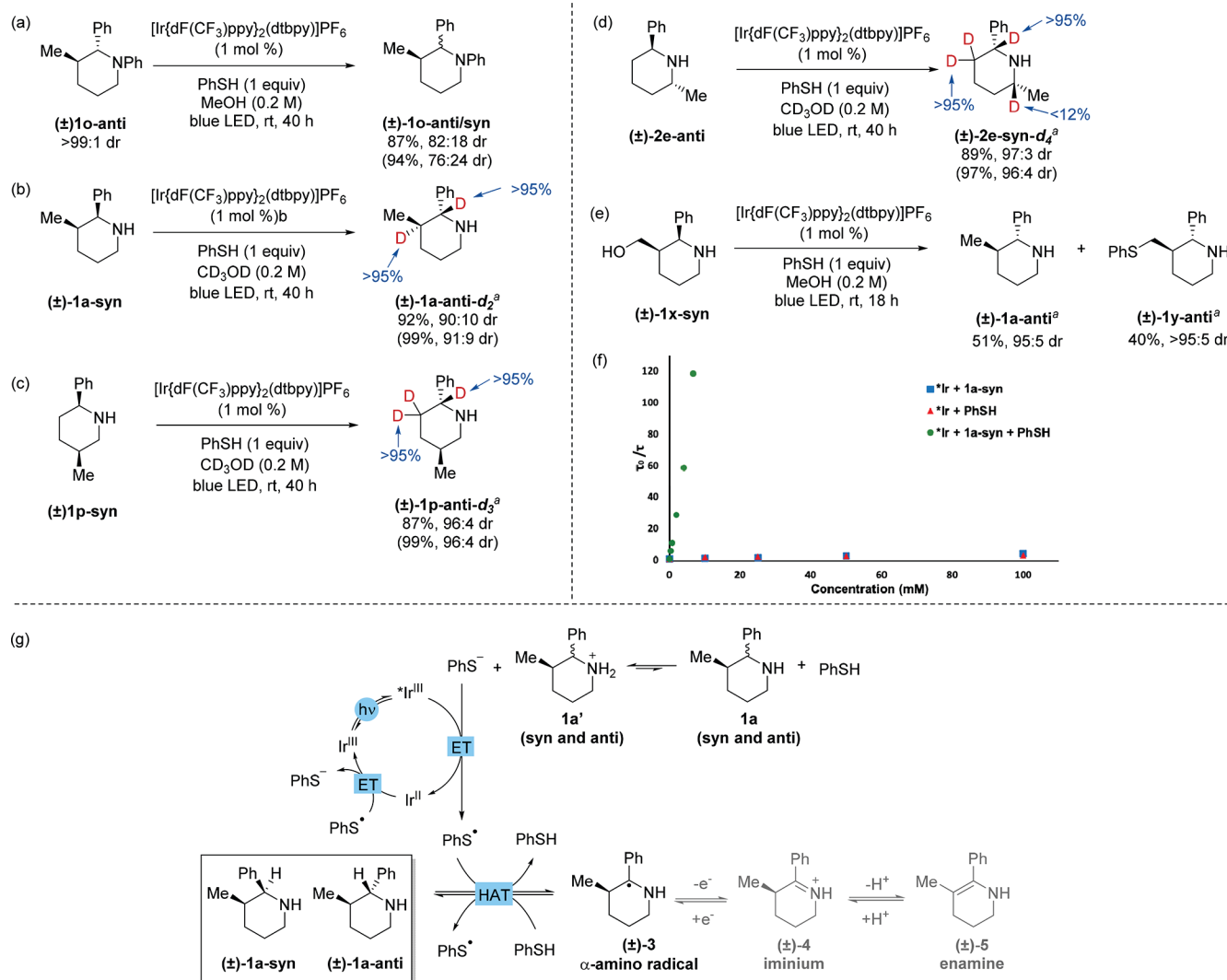


**Figure 1.** (a) Thermodynamic equilibration of **1o**. (b) Deuterium incorporation for the conversion of **1a-syn** to **1a-anti** in methanol-*d*<sub>4</sub>. (c) Deuterium incorporation for the conversion of **1p-syn** to **1p-anti** in methanol-*d*<sub>4</sub>. (d) Deuterium incorporation for the conversion of **2e-anti** to **2e-syn** in methanol-*d*<sub>4</sub>. (e) Unexpected products observed for **1x-syn**. (f) Luminescence quenching data. (g) Possible mechanism. <sup>a</sup>See footnote *a* for Table 1.

deuterium incorporation at any other sites. We hypothesize that an enamine intermediate could explain the observed deuterium incorporation at the 3-position. For **2e-anti** (Figure 1d), complete deuterium incorporation was likewise observed at the 2- and 3-positions; however, a small amount of deuterium was also incorporated at the 6-position.

The formation of an enamine intermediate is further supported by the photoredox-mediated reaction of hydroxymethylpiperidine **1x-syn**, which provided **1a-anti** and **1y-anti**, instead of the expected **1x-anti** (Figure 1e). We postulate that following enamine formation, hydroxide could be eliminated to form an  $\alpha,\beta$ -unsaturated iminium that would serve as a common intermediate to both **1a-anti** and **1x-anti** (see Figure S1 for mechanism).

To probe whether a closed-loop photoredox mechanism is plausible,<sup>13</sup> we used Scaiano's method<sup>14</sup> to determine the quantum yield of the reaction for **1a-syn**. The quantum yield was calculated to be  $\Phi = 0.1$  at early conversions, indicating that a photoredox catalyzed cycle is likely though a radical chain mechanism cannot be ruled out. UV-vis titrations confirmed that the major species in the reaction mixture is

thiophenolate, which is generated in situ by deprotonation of PhSH by piperidine **1a-syn** (see Figures S2 and S3, and Table S4). Luminescence quenching revealed that thiophenolate quenched the photocatalyst excited state more than 2 orders of magnitude faster than either PhSH or piperidine **1a-anti** did, with a bimolecular dynamic constant of  $6.6 \times 10^9 \text{ M}^{-1} \text{ s}^{-1}$  (Figure 1f, also see Figures S4–S9 and Tables S5–S7).<sup>15</sup>

A mechanistic hypothesis is depicted in Figure 1g that is consistent with the mechanistic experiments. Excitation of the iridium(III) photocatalyst produces the strongly oxidizing excited state **\*Ir<sup>III</sup>**,<sup>16</sup> which is reduced by the in situ generated thiophenolate, consistent with the more rapid quenching by the mixture of PhSH and piperidine **1a-syn** relative to either compound alone (Figure 1f).<sup>17</sup> The resulting thiophenyl radical can then undergo reversible polarity matched HAT<sup>8</sup> with piperidines **1a-syn/anti** ( $\alpha$ -amino,  $\alpha$ -methylbenzyl C–H BDE = 79–88 kcal/mol,<sup>10a,18</sup> versus PhS–H BDE = 79.0 kcal/mol<sup>19</sup>) to furnish  $\alpha$ -amino radical **3** and PhSH. Significant to this step, Bertrand et al. reported radical-mediated racemization of benzylic amines with arylthioli radicals initiated with AIBN.<sup>10a</sup> HAT between the  $\alpha$ -amino radical **3** and PhSH

then regenerates piperidines **1a**-syn/anti along with thiophenyl radical. Electron transfer from Ir(II) to the thiophenyl radical (or PhSSPh<sup>20</sup>) provides ground state Ir(III) to complete the photocatalytic cycle. The product deuteration patterns depicted in Figure 1b–d can be explained by reversible oxidation of the  $\alpha$ -amino radical intermediate **3** to iminium **4** with subsequent reversible tautomerization to enamine **5**.<sup>21</sup>

We have described the highly diastereoselective photocatalytic light-mediated epimerization of readily accessible, but contra-thermodynamic piperidines to give more stable diastereomers. Piperidines bearing a variety of substituents and substitution patterns, including substituents on the piperidine nitrogen, were effective substrates. The epimerization proceeds by a reversible process wherein either diastereomer gives the same diastereomer ratio. The observed distribution of isomers correlates reasonably well with their calculated relative stabilities, which should facilitate application of the method. In future work, we will apply this approach to the diastereoselective epimerization of other classes of heterocycles.

## ASSOCIATED CONTENT

### Supporting Information

The Supporting Information is available free of charge at <https://pubs.acs.org/doi/10.1021/jacs.0c11911>.

Experimental procedures, characterization data, crystallographic data, deuterium studies, and Cartesian coordinates of all computed structures ([PDF](#))

Crystallographic data for the picrylsulfonic acid salt of **1a**-anti ([CIF](#))

## AUTHOR INFORMATION

### Corresponding Authors

**James M. Mayer** — *Department of Chemistry, Yale University, New Haven, Connecticut 06520, United States*;  [orcid.org/0000-0002-3943-5250](https://orcid.org/0000-0002-3943-5250); Email: [james.mayer@yale.edu](mailto:james.mayer@yale.edu)

**K. N. Houk** — *Department of Chemistry and Biochemistry, University of California, Los Angeles, California 90095, United States*;  [orcid.org/0000-0002-8387-5261](https://orcid.org/0000-0002-8387-5261); Email: [houk@chem.ucla.edu](mailto:houk@chem.ucla.edu)

**Jonathan A. Ellman** — *Department of Chemistry, Yale University, New Haven, Connecticut 06520, United States*;  [orcid.org/0000-0001-9320-5512](https://orcid.org/0000-0001-9320-5512); Email: [jonathan.ellman@yale.edu](mailto:jonathan.ellman@yale.edu)

### Authors

**Zican Shen** — *Department of Chemistry, Yale University, New Haven, Connecticut 06520, United States*

**Morgan M. Walker** — *Department of Chemistry, Yale University, New Haven, Connecticut 06520, United States*

**Shuming Chen** — *Department of Chemistry and Biochemistry, University of California, Los Angeles, California 90095, United States*;  [orcid.org/0000-0003-1897-2249](https://orcid.org/0000-0003-1897-2249)

**Giovanny A. Parada** — *Department of Chemistry, Yale University, New Haven, Connecticut 06520, United States*

**Duc M. Chu** — *Department of Chemistry, Yale University, New Haven, Connecticut 06520, United States*

**Sun Dongbang** — *Department of Chemistry, Yale University, New Haven, Connecticut 06520, United States*

Complete contact information is available at: <https://pubs.acs.org/doi/10.1021/jacs.0c11911>

## Author Contributions

<sup>§</sup>Z.S. and M.M.W. contributed equally.

## Notes

The authors declare no competing financial interest.

## ACKNOWLEDGMENTS

This work was supported by NIH Grant R35GM122473 (to J.A.E.), NSF Grant CHE-1764328 (to K.N.H.), and NIH Grant R01GM050422 (J.M.M.). We thank Dr. Brandon Q. Mercado (Yale) for solving the crystal structure of **1a**-anti and Dr. Fabian Menges (Yale) for assistance with mass spectrometry. Calculations were performed on the Hoffman2 cluster at UCLA, and the Extreme Science and Engineering Discovery Environment (XSEDE), which is supported by the NSF (Grant OCI-1053575).

## REFERENCES

- (1) (a) Vitaku, E.; Smith, D. T.; Njardarson, J. T. Analysis of the Structural Diversity, Substitution Patterns, and Frequency of Nitrogen Heterocycles among U.S. FDA Approved Pharmaceuticals. *J. Med. Chem.* **2014**, *57*, 10257–10274. (b) Taylor, R. D.; MacCoss, M.; Lawson, A. D. G. Rings in Drugs. *J. Med. Chem.* **2014**, *57*, 5845–5859.
- (2) (a) Källström, S.; Leino, R. Synthesis of pharmaceutically active compounds containing a disubstituted piperidine framework. *Bioorg. Med. Chem.* **2008**, *16*, 601–635. (b) Buffat, M. G. P. Synthesis of piperidines. *Tetrahedron* **2004**, *60*, 1701–1729. (c) Bailey, P. D.; Millwood, P. A.; Smith, P. D. Asymmetric routes to substituted piperidines. *Chem. Commun.* **1998**, 633–640.
- (3) (a) Chen, W.; Paul, A.; Abboud, K. A.; Seidel, D. Rapid functionalization of multiple C–H bonds in unprotected alicyclic amines. *Nat. Chem.* **2020**, *12*, 545–550. (b) Chen, W.; Ma, L.; Paul, A.; Seidel, D. Direct  $\alpha$ -C–H bond functionalization of unprotected cyclic amines. *Nat. Chem.* **2018**, *10*, 165–169. (c) McManus, J. B.; Onuska, N. P. R.; Nicewicz, D. A. Generation and Alkylation of  $\alpha$ -Carbamyl Radicals via Organic Photoredox Catalysis. *J. Am. Chem. Soc.* **2018**, *140*, 9056–9060. (d) Millet, A.; Larini, P.; Clot, E.; Baudoin, O. Ligand-controlled  $\beta$ -selective C(sp<sup>3</sup>)–H arylation of N-Boc-piperidines. *Chem. Sci.* **2013**, *4*, 2241–2247. (e) Campos, K. R. Direct sp<sup>3</sup> C–H bond activation adjacent to nitrogen in heterocycles. *Chem. Soc. Rev.* **2007**, *36*, 1069–1084.
- (4) Walker, M. M.; Koroniewicz, B.; Chen, S.; Houk, K. N.; Mayer, J. M.; Ellman, J. A. Highly Diastereoselective Functionalization of Piperidines by Photoredox-Catalyzed  $\alpha$ -Amino C–H Arylation and Epimerization. *J. Am. Chem. Soc.* **2020**, *142*, 8194–8202.
- (5) Wiesenfeldt, M. P.; Nairoukh, Z.; Dalton, T.; Glorius, F. Selective Arene Hydrogenation for Direct Access to Saturated Carbo- and Heterocycles. *Angew. Chem., Int. Ed.* **2019**, *58*, 10460–10476.
- (6) For an example of a thermodynamically controlled radical C–H isomerization using a hypervalent iodine reagent and H<sub>2</sub>O, see: Wang, Y.; Hu, X.; Morales-Rivera, C. A.; Li, G.-X.; Huang, X.; He, G.; Liu, P.; Chen, G. Epimerization of Tertiary Carbon Centers via Reversible Radical Cleavage of Unactivated C(sp<sup>3</sup>)–H Bonds. *J. Am. Chem. Soc.* **2018**, *140*, 9678–9684.
- (7) (a) Wang, Y.; Carder, H. M.; Wendlandt, A. E. Synthesis of rare sugar isomers through site-selective epimerization. *Nature* **2020**, *578*, 403–408. (b) Shin, N. Y.; Ryss, J. M.; Zhang, X.; Miller, S. J.; Knowles, R. R. Light-driven deracemization enabled by excited-state electron transfer. *Science* **2019**, *366*, 364–369.
- (8) Dénès, F.; Pichowicz, M.; Povie, G.; Renaud, P. Thiyil Radicals in Organic Synthesis. *Chem. Rev.* **2014**, *114*, 2587–2693.
- (9) Mazzanti, A.; Lunazzi, L.; Minzoni, M.; Anderson, J. E. Rotation in Biphenyls with a Single Ortho-Substituent. *J. Org. Chem.* **2006**, *71*, 5474–5481.
- (10) (a) Escoubet, S.; Gastaldi, S.; Vanthuyne, N.; Gil, G.; Siri, D.; Bertrand, M. P. Thiyil Radical Mediated Racemization of Benzylic Amines. *Eur. J. Org. Chem.* **2006**, *2006*, 3242–3250. (b) Escoubet, S.; Gastaldi, S.; Timokhin, V. I.; Bertrand, M. P.; Siri, D. Thiyil Radical

Mediated Cleavage of Allylic C–N Bonds: Scope, Limitations and Theoretical Support to the Mechanism. *J. Am. Chem. Soc.* **2004**, *126*, 12343–12352.

(11) A phase III clinical trial was recently completed for the treatment of vasculitis with avacopan, and numerous additional clinical trials for other indications are ongoing. Avacopan's structure, bioactivity, literature, and access to ongoing clinical trials can be obtained by searching the compound name in PubChem.

(12) Loh, Y. Y.; Nagao, K.; Hoover, A. J.; Hesk, D.; Rivera, N. R.; Colletti, S. L.; Davies, I. W.; MacMillan, D. W. C. Photoredox-catalyzed deuteration and tritiation of pharmaceutical compounds. *Science* **2017**, *358*, 1182–1187.

(13) Cismesia, M. A.; Yoon, T. P. Characterizing chain processes in visible light photoredox catalysis. *Chem. Sci.* **2015**, *6*, 5426–5434.

(14) Pitre, S. P.; McTiernan, C. D.; Vine, W.; DiPucchio, R.; Grenier, M.; Scaiano, J. C. Visible-Light Actinometry and Intermittent Illumination as Convenient Tools to Study  $\text{Ru}(\text{bpy})_3\text{Cl}_2$  Mediated Photoredox Transformations. *Sci. Rep.* **2015**, *5*, 16397.

(15) In related studies, Wendlandt and coworkers observed much faster Stern–Volmer fluorescence quenching of quinuclidine and 4-bromothiophenol than either reagent alone; see Figure S8B from Wang, Y.; Carder, H. M.; Wendlandt, A. E. Synthesis of rare sugar isomers through site-selective epimerization. *Nature* **2020**, *578*, 403–408.

(16) Lowry, M. S.; Goldsmith, J. I.; Slinker, J. D.; Rohl, R.; Pascal, R. A.; Malliaras, G. G.; Bernhard, S. Single-Layer Electroluminescent Devices and Photoinduced Hydrogen Production from an Ionic Iridium(III) Complex. *Chem. Mater.* **2005**, *17*, 5712–5719.

(17) (a) Gentry, E. C.; Knowles, R. R. Synthetic Applications of Proton-Coupled Electron Transfer. *Acc. Chem. Res.* **2016**, *49*, 1546–1556. (b) Warren, J. J.; Tronic, T. A.; Mayer, J. M. Thermochemistry of Proton-Coupled Electron Transfer Reagents and its Implications. *Chem. Rev.* **2010**, *110*, 6961–7001.

(18) Luo, Y.-R. *Comprehensive Handbook of Chemical Bond Energies*; Taylor & Francis Group: Boca Raton, FL, 2007; p 104.

(19) Fu, Y.; Lin, B.-L.; Song, K.-S.; Liu, L.; Guo, Q.-X. Substituent effects on the S–H bond dissociation energies of thiophenols. *J. Chem. Soc., Perkin Trans. 2* **2002**, 1223–1230.

(20) For examples utilizing aryl disulfides as HAT reagents in photoredox catalysis, see (a) Xiang, J.-C.; Wang, Q.; Zhu, J. Radical-Cation Cascade to Aryltetralin Cyclic Ether Ligands Under Visible-Light Photoredox Catalysis. *Angew. Chem., Int. Ed.* **2020**, *59*, 21195–21202. (b) Kim, J.; Kang, B.; Hong, S. H. Direct Allylic  $\text{C}(\text{sp}^3)\text{–H}$  Thiolation with Disulfides via Visible Light Photoredox Catalysis. *ACS Catal.* **2020**, *10*, 6013–6022. (c) Patehbeieke, Y. An Overview on Disulfide-Catalyzed and -Cocatalyzed Photoreactions. *Beilstein J. Org. Chem.* **2020**, *16*, 1418–1435. (d) Nguyen, T. M.; Nicewicz, D. A. Anti-Markovnikov Hydroamination of Alkenes Catalyzed by an Organic Photoredox System. *J. Am. Chem. Soc.* **2013**, *135*, 9588–9591.

(21) (a) Leitch, J. A.; Rossolini, T.; Rogova, T.; Maitland, J. A. P.; Dixon, D. J.  $\alpha$ -Amino Radicals via Photocatalytic Single-Electron Reduction of Imine Derivatives. *ACS Catal.* **2020**, *10*, 2009–2025. (b) Trowbridge, A.; Reich, D.; Gaunt, M. J. Multicomponent synthesis of tertiary alkylamines by photocatalytic olefin-hydroaminoalkylation. *Nature* **2018**, *561*, 522–527. (c) Beatty, J. W.; Stephenson, C. R. J. Amine Functionalization via Oxidative Photoredox Catalysis: Methodology Development and Complex Molecule Synthesis. *Acc. Chem. Res.* **2015**, *48*, 1474–1484. (d) Hager, D.; MacMillan, D. W. C. Activation of C–H Bonds via the Merger of Photoredox and Organocatalysis: A Coupling of Benzylidene Ethers with Schiff Bases. *J. Am. Chem. Soc.* **2014**, *136*, 16986–16989.